

THE ELECTRONIC STRUCTURE OF THE CRONSTEDTITE LAYER

ĽUBOMÍR BENCO AND ĽUBOMÍR SMRČOK

Institute of Inorganic Chemistry, Slovak Academy of Sciences
842 36 Bratislava, Slovakia

Abstract—The bonding in a cronstedtite layer was studied using a ninefold ordered supercell band structure calculation. The tight-binding scheme based upon the extended Hückel method was used to predict the electronic structure. The size of the problem was 162 atoms with 798 valence orbitals. The calculation showed different orbital interactions of oxygen p-orbitals with neighboring atoms with respect to the position in the layer. Substitution of Fe for Si in the tetrahedra reduced the role of the valence p-orbitals of the central Fe atoms. The d-orbitals of Fe were split in accordance with the rule of t_{2g} - e_g splitting. Although the density of states at the Fermi level was high, the partially filled 3d-bands were too narrow to permit normal metallic conduction.

Key Words—Bandstructure, Cronstedtite, Density of states, Electronic structure, Extended Hückel method.

INTRODUCTION

Our understanding of the electronic structure of silicates has been enhanced by several quantum-chemical and solid-state studies. Much of the work has been done on molecules (clusters), as summarized by Gibbs (1982). Another comprehensive summary of quantum mechanical studies of Si-O and Si-F bonds in molecules and minerals has been given by Tossell (1987). The most complicated system treated so far from the mineralogical point of view (with the cluster approach) was a model of dioctahedral smectite (Aronowitz *et al* 1982), which was designed to study the isomorphous substitution of cations like Na^+ , K^+ , Mg^{2+} , Ca^{2+} and $\text{Fe}^{2+}/\text{Fe}^{3+}$ for octahedral Al^{3+} . Using the tight-binding extended Hückel method (EHT), Bleam and Hoffmann (1988a, 1988b) provided a deeper insight into the electronic structure of an infinite silicate sheet $[\text{Si}_2\text{O}_5]^{2-}$ and also addressed the problem of isomorphous substitution of Si(IV) by Al(III). Very precise *ab initio* calculation of infinite silicate layer $[\text{Si}_2\text{O}_5\text{H}_2]$ was recently published by Benco and Smrčok (1994).

Cronstedtite, a member of the kaolin family, represents a rare case: it is a compound with the same transition metal in two different coordination polyhedra. Octahedral Fe is located between a plane of hydroxyls and a silicate sheet. Si atoms are located in the centers of tetrahedra and are partially replaced by Fe atoms. The degree of substitution is not constant over samples originating from different locations. The refinement of the cronstedtite-3T structure (Smrčok *et al* 1994) has provided reliable information on the geometry and occupancies in both kinds of polyhedra in which Fe occurs.

COMPUTATIONAL DETAILS

The electronic structure calculations were done with the extended Hückel tight-binding (EHT) method

(Hoffmann 1963, Hoffmann and Lipscomb 1962, Whangbo *et al* 1979) using the Extended Hückel Molecular, Crystal and Properties Package (Whangbo *et al* 1988) and were limited to a single 1:1 cronstedtite-3T layer. The atomic parameters used for our calculations are summarized in Table 1. This kind of layer is frequently referred to as “two-dimensional” in quantum chemistry notation to emphasize that no interactions between the adjacent layers are taken into account. Positions of all non-hydrogen atoms within the layer (Table 2) were derived from the atomic coordinates given by Smrčok *et al* (1994). In the cronstedtite structure, tetrahedral positions are occupied by certain amounts of Si and Fe, dominantly by the former. For the 3T polytype described in Table 2, the occupancy factors were 86% Si and 14% Fe for both of the T sites. However, the EHT method, like other quantum chemistry methods, does not allow any “statistical” atoms or “variable” occupancies. In order to mimic the real situation in the structure a ninefold supercell was chosen in which the ratio of Si to Fe was 83.3% to 16.7%, i.e., 15 Si and 3 Fe atoms. Such a model sufficiently described the overall composition of central atoms in the tetrahedra, but there remained the problem of Fe ordering.

Only one of the possible solutions which was used in all calculations is given in Figure 1. The X-ray refinement did not provide the positions of the hydrogen atoms, so they were all positioned at a distance of 0.8 Å from the corresponding hydroxyl oxygen (Joswig and Drits 1986). All O-H bonds were oriented perpendicular to the layer pointing either to the middle of tetrahedral six-membered rings or outside the layer (Figure 2). The positions of the H atoms are not accurate, especially the position of the hydrogens bound to the cavity oxygens. Since the size of the model was, for this kind of calculation, *unusually large* (162 atoms

Table 1. Atomic parameters for extended Hückel calculations.¹

Atom	Orbital	H_{ii}	$\zeta_{ij}(c_i)$	$\zeta_{ij}(c_j)$
Fe	4s	-9.10	1.900	
	4p	-5.32	1.900	
	3d	-12.60	5.350 (0.5505)	2.000 (0.6260)
Si	3s	-17.30	1.383	
	3p	-9.20	1.383	
O	2s	-32.30	2.275	
	2p	-14.80	2.275	
H	1s	-13.60	1.300	

¹ H_{ii} s are orbital ionization energies in eV, ζ_{ij} s Slater exponents, and c_j s coefficients in the double-zeta expansion of d orbitals. From *Table of parameters for Extended Hückel Calculations*; collected by Santiago Alvarez, Barcelona, 1985.

with 798 valence orbitals), and the method itself is known not to be very sensitive to small changes in geometry (Bleam and Hoffmann 1988b), and we did not wish any "dangling" bonds, we considered our choice to be a good approximation.

The results of the electronic structure calculation are presented in terms of total and projected density of states (DOS, PDOS). DOS(E) is the number of states in the energy interval E to E + dE. Unlike molecular orbital (MO) theory in which electronic states occur at discrete energy levels the DOS represents energy levels that are spread out into bands with a characteristic width and area. Decomposition of the total DOS into bands gives the energy distribution of electronic states. Since the EHT method expresses the crystal orbitals as a linear combination of atomic orbitals (LCAO), the DOS can be partitioned into contributions made by atoms, orbitals, or linear combinations thereof. These so-called projected DOS represent the energy distributions made up of contributions from individual atoms or orbitals.

RESULTS AND DISCUSSION

Total DOS

The total DOS energy dependence of the individual cronstedtite layer is shown in the Figure 3. The total DOS consists of four main bands, s-, p-, d- and the antibonding bands, respectively. Occupied states are below the Fermi level (E_F). All bands below E_F including the d-band (intersected by this level) are split into two parts. The splitting of the bands results because band components participate in bonding states (crystal orbitals) which differ significantly in energy. The bands of the bonding region are narrow and do not overlap, their bandwidth being about 4 eV. The total DOS at Fermi level is high so cronstedtite-3T should show good electrical conductivity (Coey *et al* 1989). Nevertheless, this mineral cannot be considered a normal metallic conductor as discussed later in the PDOS Fe paragraph.

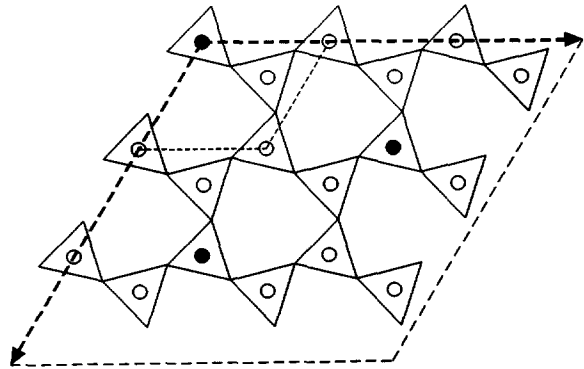


Figure 1. The computational unit cell showing the translation vectors in two dimensions. The basic unit cell of the system without iron atoms in the tetrahedral sheet is indicated in the upper left of the figure. The Fe atoms are shown as solid circles and the Si atoms as open circles.

PDOS Si

s- and p-orbital contributions from the silicon atom to the total DOS appear in Figure 4. The low electronegativity of Si atoms is responsible for the fact that these orbitals contribute to the antibonding rather than to the bonding bands. Both s- and p-orbitals contribute to both s- and p-bands as well (Figure 4). Although the amount of these contributions looks comparable, the larger portion of Si (3s) states enters the s-band and the larger portion of Si (3p) states enters the p-band.

PDOS O

The high electronegativity of O atoms caused almost all of the DOS below E_F to be due to oxygen with very small contributions to the antibonding states. Orbital contributions from the four structural types of oxygen atoms (basal, apical and hydroxyl oxygens located either in cavities or in the upper layer) to the total DOS

Table 2. Atomic coordinates in cronstedtite 3T. A1, A2 = apical oxygen atoms, O1, O2, O3 = basal oxygen atoms, T1, T2 = tetrahedrally coordinated atoms. The e.s.d.s refer to the last decimal place. Structure is hexagonal with $a = 5.497(2)$ Å, $c = 21.355(7)$ Å and the space group $P3_1$.

Atom	x	y	z
O1	0.1210(18)	0.7787(17)	0.0075(4)
O2	0.5580(17)	0.3407(18)	0.0082(4)
O3	-0.055(18)	0.2142(18)	0.0076(4)
A1	0.2258(10)	0.1102(10)	0.1160(3)
A2	0.8956(9)	0.4486(10)	0.1159(3)
T1	0.2248(6)	0.1122(6)	0.03315(7)
T2	0.8898(3)	0.4449(3)	0.03318(7)
Fe1	0.2243(2)	0.7803(2)	0.16620(5)
Fe2	0.5591(2)	0.4459(2)	0.16502(5)
Fe3	0.8935(2)	0.1149(2)	0.1650
OH1	0.5568(10)	0.7809(9)	0.1165(3)
OH2	0.8900(10)	0.7791(12)	0.2134(3)
OH3	0.5562(10)	0.1099(10)	0.2133(3)
OH4	0.2247(10)	0.4473(10)	0.2134(2)

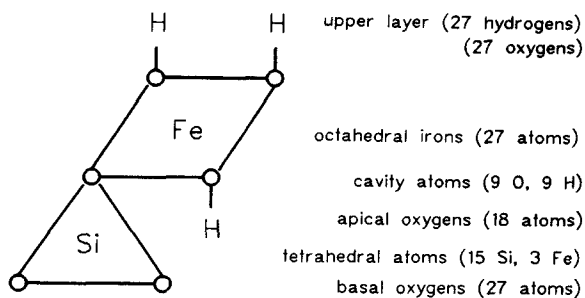


Figure 2. The scheme of the side view at the atom planes in the cronstedtite layer. Circles represent oxygen atoms tetrahedrally surrounding silicon atoms and iron atoms are placed inside octahedra. In the right side of the figure the number of atoms entering atom planes in the computational unit cell is reported.

are compared in Figure 5. To facilitate direct comparison, the DOS curves were normalized to one atom. Oxygen *s*-orbitals almost do not enter the *p*-band and vice versa, so that the *sp*-mixing of oxygen states is negligible. For basal and apical oxygen atoms the states centered at -33 eV correspond well with the position of Si (*3p*) component. Such Si (*3p*)-O (*2s*) σ bonding in a silicate sheet has already been described (Breeze and Perkins 1973, Bleam and Hoffmann 1988b). Si (*3s*) orbitals are combined with O (*2s*) orbitals into σ states appearing at about -35 eV. These states are seen in the basal O (*2s*) projected DOS. The *2s*-orbitals of apical oxygens are involved in the Si (*3s*)-O (*2s*) σ bond to a lesser extent. The position of O (*2s*) projected DOS of the hydroxyl group oxygens (cavity O and the oxygens of the upper layer) do not correspond with the position of Si *s*-components.

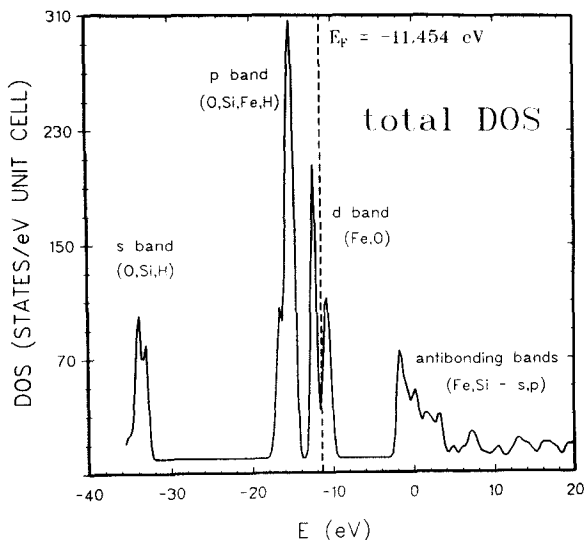


Figure 3. The total DOS of the cronstedtite layer.

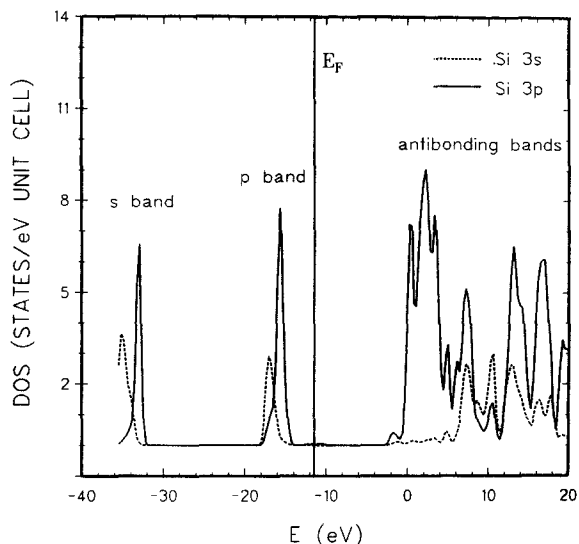


Figure 4. The projected Si (*3s*) and Si (*3p*) density of states.

The apical oxygen *p*-orbitals interact with Si (*3s*) orbitals far less than basal oxygen ones. A part of them is shifted into the *d*-band (Figure 3) instead entering not only occupied *d*-band states, but unoccupied ones, as well. The last feature is common for all oxygen atoms neighboring with iron atoms (apical, cavity and the oxygens of the upper layer). Hydroxyl oxygen *p*-orbital DOS show pronounced stabilization of a part of states not attributable to any of before-mentioned orbital interactions, which is discussed later.

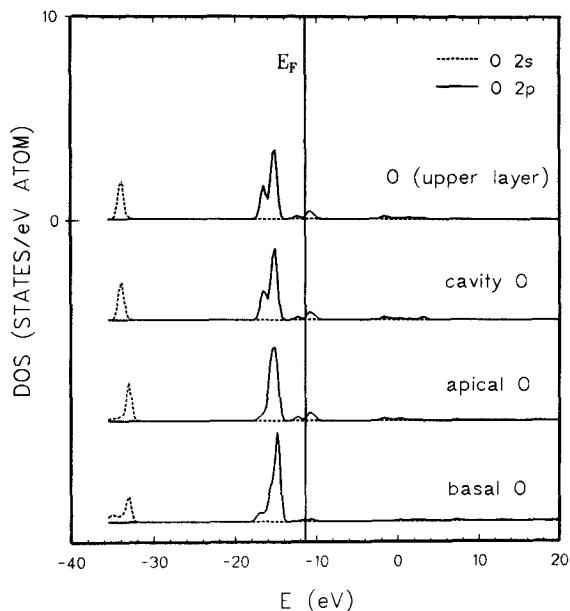


Figure 5. Comparison of the projected DOS of oxygen atoms. All data are normalized to one atom.

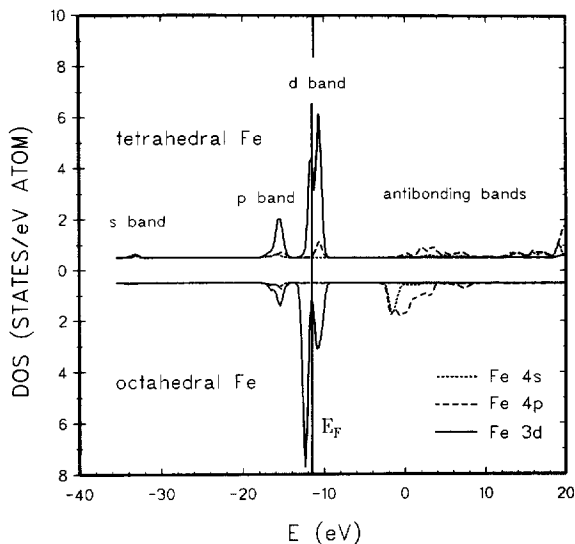


Figure 6. Comparison of the projected components of tetrahedral and octahedral iron atoms normalized to one atom.

PDOS Fe

The Fe PDOS (Figure 6) were normalized to one atom. Projected DOS for octahedral and tetrahedral Fe differ in many aspects. The s- and p-orbitals of octahedral iron atoms enter almost entirely the antibonding bands. The very small contribution to the p-band could be seen in Figure 6 and provides evidence of a small O (2p)-Fe (4s, 4p) interaction within the octahedra. On the other hand, tetrahedral s- and p-orbital contribute to every band of the bonding region. This indicates that iron atoms are involved in orbital interactions with s- and p-orbitals of basal and apical oxygens. The reason for this is the shorter tetrahedral interatomic distance and hence the larger overlap of atomic orbitals. While these are 1.71 and 1.77 Å for Fe-O (basal) and Fe-O (apical), the value for the octahedra is about 2.11 Å. Of particular interest is the comparison of the d-contributions with DOS curve. These contributions are restricted to the energy interval -18 through -9 eV (Figure 7).

Comparing the d-contributions with the p-band we see that tetrahedral iron d-orbitals are twice as engaged into the O (2p)-Fe (3d) interaction as octahedral ones. This is caused again by the larger overlap of atomic orbitals within the tetrahedra. The splitting of the d-band is in line with the rule of t_{2g} - e_g energy level splitting under the influence of the symmetrical surroundings. Though this rule has been applied to discrete energy levels, it also holds for band structures. The difference is that 3:2 is not the degeneracy ratio but the ratio of the band areas. Octahedral iron d-states are divided into two parts situated below and above the Fermi level. Both these components enter orbital

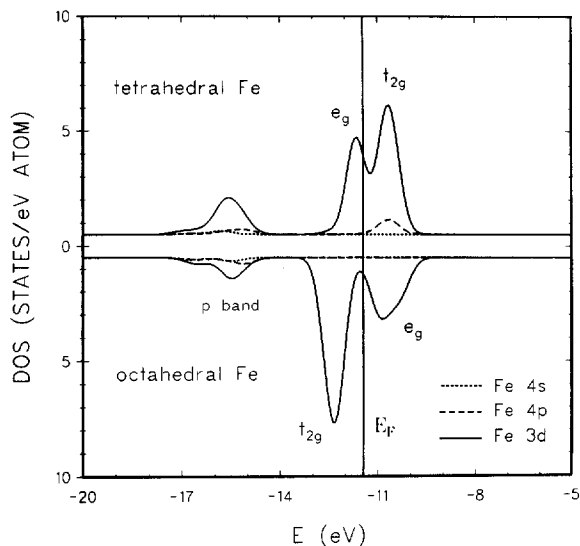


Figure 7. The projected p- and d-band components of the both types of iron atoms showing the t_{2g} - e_g splitting of the d-band.

interactions with oxygen orbitals (Figures 7 and 5). Only a small part of O (2p) states is fixed at d-band positions as expected for polar solids. The order of the tetrahedral iron d-band components is reversed, the e_g states are situated below the Fermi level while t_{2g} states are together with the Fe (4p) ones centered above the Fermi level at about -10.7 eV. The t_{2g} and e_g positions correspond again with the O-(2p) contribution to the d-band.

The width of the band is indicative of the magnitude of the orbital interactions for the electronic states within the band (Albright *et al* 1985, Hoffmann 1988, Har-

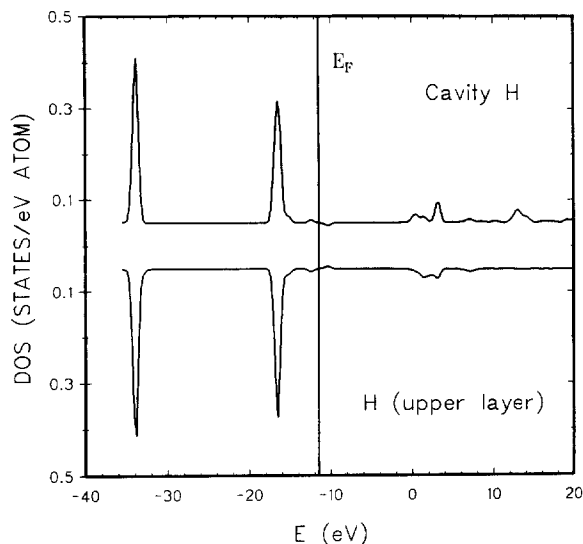


Figure 8. The projected H (1s) density of states.

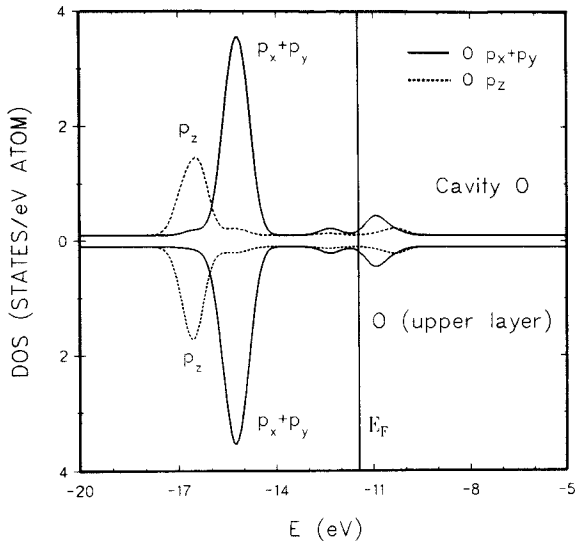


Figure 9. The comparison of the projected p-band components of the hydroxyl oxygens. All data are normalized to one atom.

risson 1980). The d-bandwidths are 3.2 eV and 3.9 eV for tetrahedral and octahedral Fe, respectively, showing larger orbital interactions of the latter. Moreover, considering the initial position of the d-atomic levels (Table 1) we see that octahedral t_{2g} states can be regarded as nonbonding whereas all others, i.e., octahedral e_g and tetrahedral t_{2g} and e_g states, can be regarded as destabilized states. The octahedral t_{2g} band being ≈ 2 eV wide is narrower than the O (2p) band of the super-degenerate non-bonded states centered at -15.3 eV (Figure 9). Such narrow bands are characteristic of localized electronic states with little orbital interaction. Though partially filled, they are so narrow that they are effectively localized and therefore cronstedtite should be a poor conductor. The relatively good conductive properties of two cronstedtite samples examined by Coey *et al* are different than those of true metals and result from the thermally activated electron hopping (Coey *et al* 1989).

PDOS H

The hydrogen s-orbital projected states (Figure 8) show the subdivision of the hydrogen s-states into s- and p-bands. Their positions are the same for the cavity hydrogen atoms and hydrogens of the upper layer hydroxyl groups. The H (1s)-O (2s) σ orbital interaction fixes both components at energies centered around the value -34.0 eV. Hydroxyl O (2s) PDOS are due to this interaction stabilized by the value of 0.5 eV compared with the tetrahedral O (2s) PDOS fixed at a higher energy level through the interaction with Si (2p) orbitals (see s-bands in the left side of Figure 5). The position of the H (1s) states in the p-bands explains

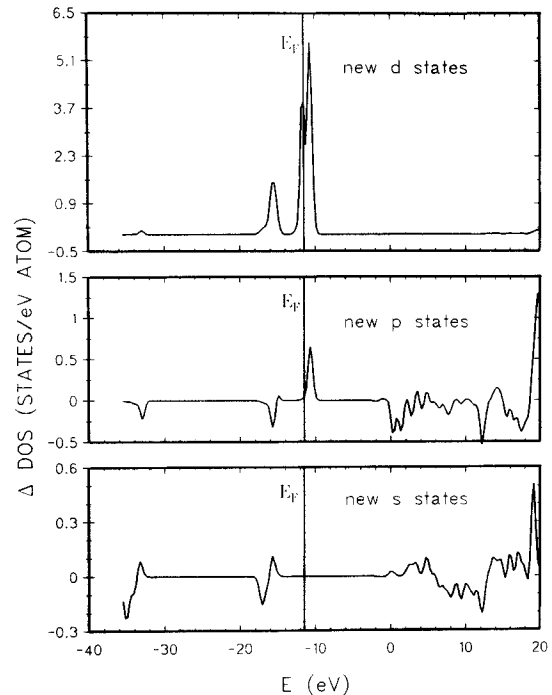


Figure 10. The differential projected DOS curves calculated for one atom inside the tetrahedra according to the relation (DOS Fe – DOS Si). The curves show which states disappear and which ones appear after silicon-by-iron replacement.

the stabilization shift in the hydroxyl oxygen p-band. Figure 9 is an excellent example of the effect of symmetry on orbital interactions. The proton 1s-orbital cannot interact with O $2p_x$, $2p_y$ -orbitals because of symmetry, whereas this symmetry restriction does not apply to H 1s-O $2p_z$ orbital interactions.

Isomorphous Fe-for-Si substitution

The electronic structure changes caused by isomorphous Fe for Si substitution are documented in Figure 10. Keeping the whole system unchanged except for the above-mentioned substitution we subtracted the PDOS curves, writing symbolically PDOS(Fe, Si) – PDOS(Si) (simplified). The differential PDOS curves represent created and/or annihilated states (located above or below the zero line) arising from Fe for Si substitution. All d-states are of course new. They enter orbital interactions with tetrahedral oxygen atoms contributing therefore to s-, p- and d-bands. As it was mentioned above p-orbital bonding interactions of the iron atoms are lowered compared with the Si (3p) orbital interactions. The much smaller energy difference between the orbital energies of the O (2p) and Fe (3d) orbitals than O (2p) and Fe (4p) orbitals (Table 1) caused the Fe (4p) orbitals to be replaced in bonds by Fe (3d) orbitals. The contribution of Fe 4p orbitals is shifted from the bonding region to the position just

above the Fermi level. The s-orbitals of Fe atoms play the same role as those of silicon atoms, but the energy levels they contribute to are shifted towards higher energies.

CONCLUSIONS

Though the calculations were done just for one possible ordered Si/Fe configuration, the size of the computational unit cell allows generalizations for all configurations but the scheme with neighbouring Fe/Fe atoms in tetrahedra. (1) The theoretical investigation of the cronstedtite layer shows different orbital interactions of oxygen p-orbitals depending on their position in the layer. (2) The bands with hydrogen orbitals have a strong stabilizing effect on oxygen p-orbital bonding. (3) Iron atom d-orbitals show pronounced splitting consistent with the rule of t_{2g} - e_g splitting under the influence of the symmetrical surroundings. (4) The isomorphous substitution of tetrahedral Si by Fe atoms reduces the role of central atom p-orbitals in chemical bonding. They are replaced by iron d-orbitals, a considerable part of which is included into the p-band.

ACKNOWLEDGMENTS

We are very grateful to P.C. Burns and one anonymous referee for stimulating comments. This work was financially supported by a research grant 02/86/92 of the Grant Agency of the Slovak Academy of Sciences.

REFERENCES

- Albright, T. A., J. K. Burdet, and M.-H. Whangbo. 1985. *Orbital Interactions in Chemistry*. New York: Wiley-Interscience Pub., 229–257.
- Aronowitz, S., L. Coyne, J. Lawless, and J. Rishpon. 1982. Quantum-chemical modeling of smectite clays. *Inorg. Chem.* **21**: 3589–3593.
- Benco, L., and L. Smrčok. 1994. *Ab initio* calculated electron densities for tetrahedral sheet $[H_2Si_2O_5]_{\infty}$ in phyllosilicates. *Phys. Chem. Miner.* **21**: 401–406.
- Bleam, W. F., and R. Hoffmann. 1988a. Isomorphous substitution in phyllosilicates as an electronegativity perturbation: Its effect on bonding and charge distribution. *Inorg. Chem.* **27**: 3180–3186.
- Bleam, W. F., and R. Hoffmann. 1988b. Orbital interactions in phyllosilicates: Perturbations of an idealized two-dimensional, infinite silicate frame. *Phys. Chem. Miner.* **15**: 398–408.
- Breeze, A., and P. G. Perkins. 1973. Energy band structure of silica. *J. Chem. Soc. Faraday Trans. II* **69**: 1237–1242.
- Coey, J. M. D., T. Bakas, C. M. McDonagh, and F. J. Litters. 1989. Electrical and magnetic properties of cronstedtite. *Phys. Chem. Miner.* **16**: 394–400.
- Gibbs, G. V. 1982. Molecules as models for bonding in silicates. *Amer. Miner.* **67**: 421–450.
- Harrison, W. A. 1980. *Electronic Structure and the Properties of Solids*. San Francisco: Freeman Press, 34.
- Hoffmann, R. 1963. An extended Hückel theory. I. *Hydrocarbons. J. Chem. Phys.* **39**: 1397–1412.
- Hoffmann, R., and W. N. Lipscomb. 1962. Theory of polyhedral molecules. I. Physical factorizations of the secular equation. *J. Chem. Phys.* **36**: 2179–2189.
- Hoffmann, R. 1988. *Solids and Surfaces*. New York: VCH Pub. Inc., 7–8.
- Joswig, W., and V. A. Drits. 1986. The orientation of the hydroxyl groups in dickite by X-ray diffraction. *N. Jb. Miner. Mh.* **1986**: 19–22.
- Smrčok, L., S. Đurovič, V. Petříček, and Z. Weiss. 1994. Refinement of the crystal structure of cronstedtite 3T. *Clays & Clay Miner.* **42**: 544–551.
- Tossell, J. A. 1987. Quantum mechanical studies of Si-O and Si-F bonds in molecules and minerals. *Phys. Chem. Miner.* **14**: 320–326.
- Whangbo, M. H., R. Hoffmann, and R. B. Woodward. 1979. Conjugated one and two dimensional polymers. *Proc. R. Soc. London Ser. A* **366**: 23–46.
- Whangbo, M. H., M. Evain, T. Hungbanks, M. Kertesz, S. D. Wijeyesekera, C. Wilker, C. Zheng, and R. Hoffmann. 1988. Extended Hückel Molecular, Crystal and Properties Package. QCPE Program No. 571, Indiana University.

(Received 25 February 1993; accepted 1 March 1994; Ms. 2340)